Ionization dynamics and gauge invariance

J. Vábek [1,2,3] H. Bachau [1,*] and F. Catoire [1,†]

[1]*Centre Lasers Intenses et Applications, Université de Bordeaux–Centre National de la Recherche Scientifique–CEA, 33405 Talence Cedex, France*

[2]*ELI Beamlines Centre, Institute of Physics, Czech Academy of Sciences, Za Radnicí 835, 25241 Dolní Břežany, Czech Republic*

[3]*Czech Technical University in Prague, Faculty of Nuclear Sciences and Physical Engineering, Jugoslávských Partyzánů 1580/3, 160 00 Praha 6, Czech Republic*

(Received 19 May 2022; accepted 4 November 2022; published 28 November 2022)

Photoionization is one of the most fundamental processes in laser-matter interaction. It plays a crucial role also from the practical point of view since the electron-density dynamics in a gaseous medium is a process that affects the field propagation. Photoionization has been addressed in different regimes: linear, multiphoton, and tunneling. The ideal tool that allows for the description of ionization, in all aforementioned regimes, is the numerical evaluation of the time-dependent Schrödinger equation. The determination of the electron density needs the computation of the time-dependent ionization probability which unfortunately is an ambiguous quantity due to the gauge dependence of the latter. In this paper, we show how to overcome this difficulty by properly defining the time-dependent ionization probability in the context of the resolvent operator method. We show in particular that the velocity gauge allows for a definition of adiabatic states that is suitable to define an ionization threshold at all times during the interaction to compute ionization probability. Applications to linear, multiphoton, and tunneling regimes are presented for the one-dimensional problem. The extension to the nondipole case is discussed and we show that time-dependent ionization probability cannot be defined unambiguously due to the introduction of the magnetic-field component. We also discuss the case of gauge invariance in a subspace of the eigenbasis defined by the Hamiltonian.

DOI: 10.1103/PhysRevA.106.053115

I. INTRODUCTION

Photoionization is an ideal tool to investigate the fundamental properties of laser-matter interaction. In particular, historically it revealed the quantum nature of light (i.e., existence of photons) and matter. Over the years different regimes of photoionization have been investigated. The linear regime, for which one photon is absorbed leading to ionization, has been thoroughly studied in atoms, molecules, and solids. In the case of photoemission from solids it allows for the study of band structure [1] and in the case of atoms and molecules the target wave function can be extracted [2]. Ionization in the multiphoton regime has been an important step for the study of nonlinear physics [3] up to the strong-field ionization regime. The latter was a real breakthrough with the emergence of high-order harmonic generation [4], and the field of attoscience is one of the outcomes [5]. The study of the photoionization in a pump-probe scheme also allows the determination of the Wigner delay in atomic systems [6–9]. More recently, photoionization by strong Extreme ultraviolet (XUV) field reveals the contribution of the nondipole effects in the photoionization spectra in both the linear [10] and nonlinear regimes [11,12].

From the theoretical point of view, the computation of photoelectron spectra (PES) can be obtained with high accuracy and fidelity when compared to experimental results. Nevertheless, the fundamental aspect of the time evolution of the ionization process remains out of reach because of the lack of a proper observable which, as usually defined, becomes gauge dependent. This is understood from the fundamental point of view and is not stemming from an inaccuracy inherent to solving the Schrödinger equation unlike for the strong-field approximation [13,14].

From the experimental point of view, the pump-probe scheme can be employed in order to study the dynamics of the ionization process [15]. It consists in using a first pulse in order to trigger the process and after some time to use another laser field to study the perturbation of the system induced by the first one. The physical mechanism that is used as a probe is for instance the second ionization which will probe the single ionization dynamics. From this point of view, one obtains the ionization probability as a function of time referring to the delay between the two pulses. Although the delay has a dimension of time, it is only a *parameter* of the Hamiltonian and not its *variable*. In this sense, the delay does not play the same role as the time related to the proper evolution of the system being excited by the pump pulse. As a matter of fact, computing the ionization probability as a function of the pump-probe delay is a gauge invariant quantity. Retrieving the probability of ionization as a function of time is of prime interest when one wants to investigate the dynamics

*Present address: BP 119, 49 Cours Pasteur, 33000 Bordeaux, France.

†fabrice.catoire@u-bordeaux.fr

of single ionization. Moreover, from the practical point of view the determination of ionization probability allows one to infer the electron density created in the medium which can be used for other purposes such as light propagation for instance when it is coupled with the Maxwell equation [16], and more generally for further classical analysis [17]. In most of the numerical studies where time-dependent electron density is needed, a rate equation is used [18,19]. These equations rely on a large number of hypotheses, and in particular incoherence of the ionization process as well as adiabaticity [20]. The purpose of this paper is to provide a theoretical framework which will allow expressing the time-dependent ionization probability in a physically meaningful form when analyzing the energy distribution defined by the wave-packet solution of the time-dependent Schrödinger equation (TDSE). This study will be performed by means of the resolvent operator [21–23]. The paper is organized as follows.

(i) First we describe our standpoint in order to provide insights of what is the proper procedure to extract the time-dependent ionization probability.

(ii) Then we apply this procedure in the case of one-photon ionization, multiphoton ionization, and tunneling regimes.

(iii) Finally, we discuss its applicability in the case of nondipole description of the field and in the case of Hamiltonian subspace propagation.

Single active electron approximation (SAEA), as well as atomic units, will be used unless otherwise stated.

II. CONSTRUCTION OF THE TIME-DEPENDENT IONIZATION PROBABILITY

The Hamiltonian describing the interaction of an electromagnetic field in the frame of the SAEA is written

$$\begin{aligned} H_{\mathfrak{g}}(t) &= \tfrac{1}{2}[\boldsymbol{P} - q\boldsymbol{A}(\boldsymbol{r},t)]^2 + q\phi(\boldsymbol{r},t) + V(\boldsymbol{r}) \\ &= H_0 + V_{I,\mathfrak{g}}(t). \end{aligned} \tag{1}$$

Here q is the charge of the electron ($q=-1$) interacting with the local effective potential $V(\boldsymbol{r})$ describing the system composed of the other $N-1$ electrons. H_0 is the field-free Hamiltonian (set by $\boldsymbol{A}=0$ and $\phi=0$) and $V_{I,\mathfrak{g}}(t)$ is the interaction potential provided in the gauge $\mathfrak{g}$. The interaction provided in gauge $\mathfrak{g}$ is described by the vector potential $\boldsymbol{A}(\boldsymbol{r},t)$ and the scalar potential $\phi(\boldsymbol{r},t)$. The magnetic and electric fields, in this frame, are written

$$\begin{aligned} \mathcal{B}(\boldsymbol{r},t) &= \boldsymbol{\nabla}\times\boldsymbol{A}(\boldsymbol{r},t), \\ \mathcal{E}(\boldsymbol{r},t) &= -\frac{\partial\boldsymbol{A}(\boldsymbol{r},t)}{\partial t} - \boldsymbol{\nabla}\phi(\boldsymbol{r},t). \end{aligned} \tag{2}$$

As it is well known, one can transform the vector and scalar potentials keeping the electric and magnetic fields unchanged. The relation between transformed and original potentials is expressed as

$$\begin{aligned} \boldsymbol{A}'(\boldsymbol{r},t) &= \boldsymbol{A}(\boldsymbol{r},t) + \boldsymbol{\nabla}\chi(\boldsymbol{r},t), \\ \phi'(\boldsymbol{r},t) &= \phi(\boldsymbol{r},t) - \frac{\partial\chi(\boldsymbol{r},t)}{\partial t}, \end{aligned} \tag{3}$$

where $\chi(\boldsymbol{r},t)$ is an arbitrary function of $\boldsymbol{r}$ and t. From the vector and scalar potentials expressed in the new gauge $\mathfrak{g}'$, the corresponding Hamiltonian is provided by

$$H_{\mathfrak{g}'} = \tfrac{1}{2}[\boldsymbol{P} - q\boldsymbol{A}'(\boldsymbol{r},t)]^2 + q\phi'(\boldsymbol{r},t) + V(\boldsymbol{r}). \tag{4}$$

One can also express the gauge transformation of the Hamiltonian as

$$H_{\mathfrak{g}'} = UH_{\mathfrak{g}}U^{\dagger} - q\frac{\partial\chi(\boldsymbol{r},t)}{\partial t}, \tag{5}$$

with U being the unitary transformation given by $U = e^{iq\chi(\boldsymbol{r},t)}$. In particular, local potentials remain unchanged under the gauge transformation. Correspondingly, the transformation of the ket solution of the TDSE satisfies

$$|\Psi_{\mathfrak{g}'}(t)\rangle = U|\Psi_{\mathfrak{g}}(t)\rangle. \tag{6}$$

$|\Psi_{\mathfrak{g}}(t)\rangle$ and $|\Psi_{\mathfrak{g}'}(t)\rangle$ are solutions of the TDSE for the Hamiltonian expressed in the $\mathfrak{g}$ and $\mathfrak{g}'$ gauges, respectively.

There are physical quantities that are gauge invariant, meaning that they are the same irrespective of the choice of gauge in which the wave function is expressed. We can recall a few of them: the position operator, the kinetic momentum, and also the current defined as $\boldsymbol{j} = \frac{1}{2}[\Psi^*\boldsymbol{\Pi}\Psi + \Psi\boldsymbol{\Pi}^*\Psi^*]$ with $\boldsymbol{\Pi} = -i\boldsymbol{\nabla} - q\boldsymbol{A}$. In the length gauge and dipole regimes, $\boldsymbol{\Pi}$ reduces to $-i\boldsymbol{\nabla}$. This means, in particular, that the harmonic spectrum, defined as the Fourier transform of the current, is gauge invariant as is the electron density in accordance with the continuity equation. Actually, the electron density is sometimes used to define the time-dependent ionization probability [24]. The density is then integrated in a given volume, large enough to include all the wave function at time $t=0$, and plotted as a function of time. While this quantity is indeed gauge invariant, it depends on the parameters defining the volume of integration and thus cannot be used as a reference quantity to compute the time-dependent ionization probability. A different procedure must then be defined.

Generally speaking, the PES are calculated by projecting the wave function obtained at the end of the interaction with an electromagnetic field on the states $|\varphi^-(\boldsymbol{k})\rangle$. The latter states correspond to the field-free eigenstates of the field-free Hamiltonian H_0 having an eigenenergy E defined in the continuum ($E>0$) and characterized by the momentum $\boldsymbol{k}$ so that $E=\frac{k^2}{2}$. These states also have the proper incoming properties as indicated by the minus sign and being normalized in momentum [25,26]. Having defined these states, one can construct the ionization probability operator as $\hat{P}_I = |\varphi^-(\boldsymbol{k})\rangle\langle\varphi^-(\boldsymbol{k})|$. The differential in energy and angle PES is then

$$\frac{d\mathcal{P}_{\mathfrak{g}}}{d\boldsymbol{k}} = \langle\Psi_{\mathfrak{g}}(T_f)|\hat{P}_I|\Psi_{\mathfrak{g}}(T_f)\rangle, \tag{7}$$

with $\Psi_{\mathfrak{g}}(T_f)$ being the wave function obtained at the end of the pulse ($t=T_f$) when solving the TDSE in the gauge $\mathfrak{g}$. The probability of ionization at the end of the pulse is then simply provided by

$$\mathcal{P}_{I,\mathfrak{g}} = \int d\boldsymbol{k}\frac{d\mathcal{P}_{\mathfrak{g}}}{d\boldsymbol{k}}. \tag{8}$$

If the TDSE is solved in another gauge $\mathfrak{g}'$, due to the fact that $\chi(\boldsymbol{r},t>T_f)=0$, the quantities defined by Eqs. (7) and (8) are identical under the gauge transformation. Using the closure relation, it is clear that ionization probability can also be expressed as $\mathcal{P}_{I,\mathfrak{g}} = 1 - \mathcal{P}_{\text{bound},\mathfrak{g}}$ with $\mathcal{P}_{\text{bound},\mathfrak{g}} =$

$\sum_n |\langle n|\Psi_{\mathfrak{g}}(T_f)\rangle|^2$ being the probability of remaining in the bound states noted $|n\rangle$, ground state included.

How can one extend this definition of ionization that would apply for any time? One would be tempted to simply generalize the above formula by defining $\mathcal{P}_{I,\mathfrak{g}}(t) = \int d\boldsymbol{k}\langle\Psi_{\mathfrak{g}}(t)|\hat{P}_I|\Psi_{\mathfrak{g}}(t)\rangle$. Unfortunately, this quantity is not gauge invariant at any time since $\mathcal{P}_{I,\mathfrak{g}}(t) \neq \mathcal{P}_{I,\mathfrak{g}'}(t)$ in general even though there is equality for $t \geqslant T_f$ as mentioned in the previous paragraph. The physical reason of this inequality stems from the definition of the ionization operator using a projection on states defined for the field-free Hamiltonian. Nevertheless, one can infer the probability of ionization from one gauge to another at any time. By transforming the operator $\hat{P}_{I,\mathfrak{g}}$, used to calculate the ionization probability in a gauge $\mathfrak{g}$, into $\hat{P}_{I,\mathfrak{g}'} = U\hat{P}_{I,\mathfrak{g}}U^\dagger$ then the same probability is obtained at any time when the projection is performed on the transformed wave function. Despite the fact that one can link the observables expressed in different gauges, it remains that the results are not identical at any time in the two gauges. In order to define unambiguously the time-dependent ionization probability, we rely on the properties of the transformed Hamiltonian. In the field-free case, the ionization threshold is clearly attributed to $E = 0$, but when the interaction with the electromagnetic field is turned on, this definition of ionization threshold is no longer true in general.

In order to solve this dilemma, we use the resolvent operator defined as

$$R_{H_0}(E) = N_\epsilon \frac{\epsilon^2}{(E - H_0)^2 + \epsilon^2}. \tag{9}$$

This operator is the one defined in [21,22] where the field-free Hamiltonian H_0 is detailed in Eq. (1). N_ϵ is a coefficient used to define the probability density in energy for a fixed given value of ϵ. In Appendix A we recall the main properties of the resolvent. Briefly, it is an operator projecting onto the continuum eigenstates of energy E defined by H_0. Here the resolvent is described by the second-order expression since only the low-energy distribution will be studied in this paper, but there is no limitation to extend it to higher order. The ϵ parameter is numerically set to a finite value but the limit $\epsilon \to 0$ transforms the operator into a distribution that is the consequence of the residue theorem [27]. More practically, there exists a range of epsilon for which Eq. (9) does not depend on the latter parameter (see for instance [21,22]). According to this definition, the calculation of

$$\int_{E>0} dE\,\langle\Psi_{\mathfrak{g}}(T_f)|R_{H_0}(E)|\Psi_{\mathfrak{g}}(T_f)\rangle \tag{10}$$

provides the ionization probability $\mathcal{P}_{I,\mathfrak{g}}$ defined by Eq. (8) and is gauge independent as demonstrated earlier.

The novel aspect of our formulation is to extend this approach by using a time-dependent Hamiltonian. We then define the time-dependent resolvent operator as

$$R_{H_{\mathfrak{g}}(t)}(E) = N_\epsilon \frac{\epsilon^2}{[E - H_{\mathfrak{g}}(t)]^2 + \epsilon^2}, \tag{11}$$

where $H_{\mathfrak{g}}(t)$ is the time-dependent Hamiltonian as defined by Eq. (1) in a given gauge $\mathfrak{g}$. From this definition, the integration over $E > 0$ then would provide the ionization probability. Nevertheless, the energy $E = 0$ has to correspond to a physically meaningful quantity, namely, the threshold energy defined for field-free electron energy in the continuum as detailed earlier. Unfortunately the latter property relies on the definition of the field-free Hamiltonian and spectrum. The fundament of our approach is then to cope with a transformation of the time-dependent Hamiltonian that keeps the spectrum identical to the field-free Hamiltonian one. We start with the theorem stating that an eigenstate $|\Psi_E\rangle$ of the Hamiltonian H associated with the eigenenergy E defines the same eigenvalue equation for the new eigenstate $T|\Psi_E\rangle$, referred to as the adiabatic state, with the new Hamiltonian $THT^\dagger$ and the *same energy* E (see Appendix B for more details and demonstration). T is a unitary operator defined as $e^{if(\boldsymbol{r},t)}$ with f a real function of $\boldsymbol{r}$ and t. Note that the aforementioned transformation is not an operation transforming the Hamiltonian from one gauge to another as defined in Eq. (5). Starting from this theorem, one just needs to find a Hamiltonian written as $TH_0T^\dagger$ corresponding to the actual Hamiltonian when the field is on. If we restrict our paper to the case of dipole approximation, such a Hamiltonian exists and it is provided by the so-called velocity gauge. Indeed, in that gauge the Hamiltonian is written $H_V(t) = \frac{[\boldsymbol{P}+\boldsymbol{A}(t)]^2}{2} + V(\boldsymbol{r}) = TH_0T^\dagger$ with $T = e^{-i\boldsymbol{A}(t)\cdot\boldsymbol{r}}$. Note that the operator T acts as a translation of the states by $\boldsymbol{A}(t)$ in the momentum space. From this statement, we can now use the velocity gauge in the resolvent frame in order to define the resolvent operator as

$$R_{H_V(t)}(E) = N_\epsilon \frac{\epsilon^2}{[E - H_V(t)]^2 + \epsilon^2}. \tag{12}$$

The time-dependent ionization probability density is then

$$\mathcal{P}_I(E,t) = \langle\Psi_V(t)|R_{H_V(t)}(E)|\Psi_V(t)\rangle \tag{13}$$

with $|\Psi_V(t)\rangle$ the ket solution of the TDSE in the velocity gauge. The time-dependent ionization probability is given by

$$\mathcal{P}_I(t) = \int_{E>0} dE\,\langle\Psi_V(t)|R_{H_V(t)}(E)|\Psi_V(t)\rangle. \tag{14}$$

The property $H_V(t) = TH_0T^\dagger$ can now be used to rewrite Eq. (14) into

$$\mathcal{P}_I(t) = \int_{E>0} dE\,\langle\Psi_V(t)|N_\epsilon \frac{\epsilon^2}{(E - TH_0T^\dagger)^2 + \epsilon^2}|\Psi_V(t)\rangle. \tag{15}$$

Taking the T operator out of the denominator we get

$$\mathcal{P}_I(t) = \int_{E>0} dE\,\langle\Psi_V(t)|T^\dagger R_{H_0}(E)T|\Psi_V(t)\rangle. \tag{16}$$

Since $T|\Psi_V(t)\rangle = |\Psi_L(t)\rangle$ by virtue of the Goeppert-Mayer transform [28], where $|\Psi_L(t)\rangle$ is the ket solution of the TDSE in the length gauge, we get

$$\mathcal{P}_I(t) = \int_{E>0} dE\,\langle\Psi_L(t)|R_{H_0}(E)|\Psi_L(t)\rangle. \tag{17}$$

This means that the ionization probability can be obtained by projecting on the states defined in the length gauge. In

particular we have

$$\mathcal{P}_I(t) = \int_{E>0} dE \langle \Psi_L(t)|R_{H_0}(E)|\Psi_L(t)\rangle = 1 - \sum_n |\langle n|\Psi_L(t)\rangle|^2, \quad (18)$$

which allows one to define the ionization probability only by projecting on the bound states ($|n\rangle$). This procedure will be referred to as the bound-state projection (BSP) in the following.

In conclusion of this section, the time-dependent ionization probability can be obtained with an unambiguous physical meaning. In particular, we have shown that the velocity gauge defined in the dipole approximation characterizes a Hamiltonian having a spectrum which is the same as the one defined for the field-free Hamiltonian. Using the resolvent operator method (ROM) it is then easy to retrieve the energy resolved ionization probability. We also have shown by means of the ROM that the wave function expressed in the length gauge is physically meaningful and thus can be projected on the field-free states in order to define the time-dependent ionization probability. This analysis has been done in the frame of the ROM since it helps in getting an easier physical sense. However, the same results would have been obtained by projecting onto the adiabatic states defined by the exact incoming wave functions on which the operator T has been applied (see Appendix B). The use of the ROM avoids this step which can be cumbersome.

In the next sections, we will apply the general approach previously presented in cases corresponding to physical conditions of interest: one-photon ionization, multiphoton ionization, and finally tunneling regimes. All calculations will be done using the SAEA and in one dimension since extending the application in full dimension, much more involved from the computational point of view, will not bring any further information for our purposes.

III. NUMERICAL STUDY IN DIFFERENT REGIMES

The Hamiltonian is modeled by using the one-dimensional soft-core potential $[V(x) = -\frac{1}{\sqrt{a^2+x^2}}]$ with parameter $a = 1$ a.u. providing a ground state with energy $E_0 = -0.671$ a.u (i.e., -18.25 eV). The TDSE is solved using the Crank-Nicolson propagator. The wave function is described by the grid-method using a sixth-order finite difference element using the Numerov description with $dx = 0.4$ a.u. in a box of dimension $x_{\max} = 100$ a.u. The TDSE is solved in the velocity gauge and the vector potential is given by

$$A(t) = A_0 \cos(\omega_0 t) \sin^2\left(\pi \frac{t}{T_f}\right), \quad (19)$$

so that $A(t=0) = A(t=T_f) = 0$ imposing $\chi(\boldsymbol{r}, t = T_f) = 0$ and $T_f = N\frac{2\pi}{\omega_0}$ is the total pulse duration with N the number of cycles of the laser pulse. We defined $A_0 = \frac{\mathcal{E}_0}{\omega_0}$ with $\mathcal{E}_0$ being the amplitude of the electric-field envelope. The electric field is provided by $\mathcal{E}(t) = -\frac{\partial A(t)}{\partial t}$. The transformation from velocity to length gauge is straightforward in one dimension and is provided by Eq. (6).

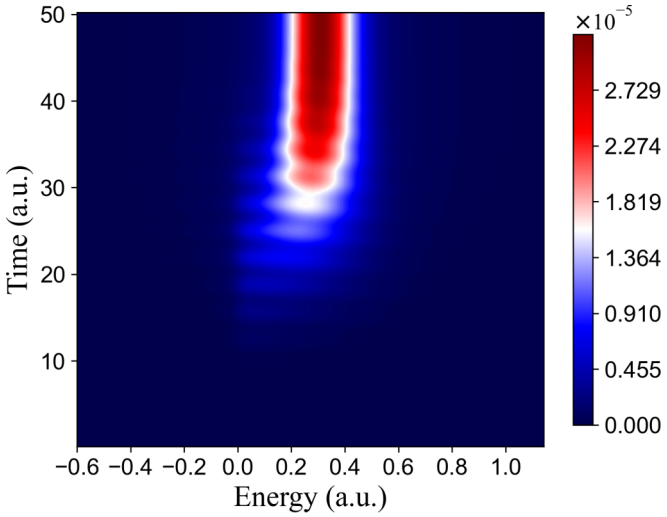

FIG. 1. Plot of the time-dependent probability density resolved in energy as defined by Eq. (13) (linear scale). The field is set with an amplitude of $\mathcal{E}_0 = 0.01$ a.u., a central frequency of $\omega_0 = 1$ a.u., and a pulse duration of eight cycles.

The previous model will be applied in three different regimes: (i) one-photon ionization, (ii) two-photon ionization by decreasing the photon energy, and (iii) the tunneling regime by decreasing the photon energy and increasing the field intensity.

A. Linear regime

In this section we set the frequency of the fundamental field to $\omega_0 = 1.0$ a.u. ($\lambda = 45.61$ nm) and a field amplitude $\mathcal{E}_0 = A_0 \times \omega_0 = 1.0 \times 10^{-2}$ a.u. (i.e., $I_0 = 3.5 \times 10^{12}$ W/cm^2). The ponderomotive energy ($U_p = \frac{A_0^2}{4}$) is 2.5×10^{-5} a.u. and the Keldysh parameter ($\gamma = \sqrt{\frac{-E_0}{2U_p}}$) is $\gamma = 115 \gg 1$ in this regime. Such a low peak amplitude of the electric field leads to a linear response of the ionization process. We can compute the ionization probability as defined by Eq. (13) as a function of time and energy. The total pulse duration is set to eight optical cycles. The resolvent, expressed in the velocity gauge which is the gauge used for the TDSE propagation, is computed for the order 2 and a resolution $\epsilon = 3 \times 10^{-2}$ a.u. These parameters of the resolvent are kept the same hereafter unless otherwise stated. The results are presented in Fig. 1.

We checked numerically that the probability of ionization expressed by Eq. (13), using the wave function and the resolvent in the velocity gauge, provides the same results as using the wave function in the length gauge expressed by the integrant of Eq. (17) using the field-free Hamiltonian in the ROM. From the first-order perturbation theory, one expects to obtain an energy distribution presenting a peak centered at $E = 0.328$ a.u. at the end of the interaction and the peak width inversely proportional to the pulse duration.

From the results of Fig. 1, we observe the evolution of the energy distribution which appears as a peak centered at 0.2 a.u. at the beginning of the pulse and then deviates to larger energy and finally reaches the value of 0.328 a.u. at

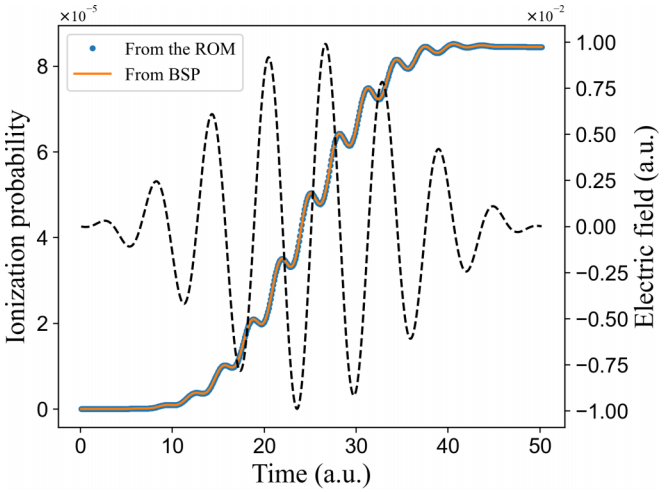

FIG. 2. Plot of the ionization probability as a function of time. This is the result of the integration over energy of the probability density obtained in Fig. 1 and as defined by Eq. (14). The results are presented by the dotted blue line. The black dashed line is the time evolution of the electric field. The full orange curve is the result obtained by removing the bound states [BSP; see Eq. (18)] when the wave function is expressed in the length gauge as detailed in the text.

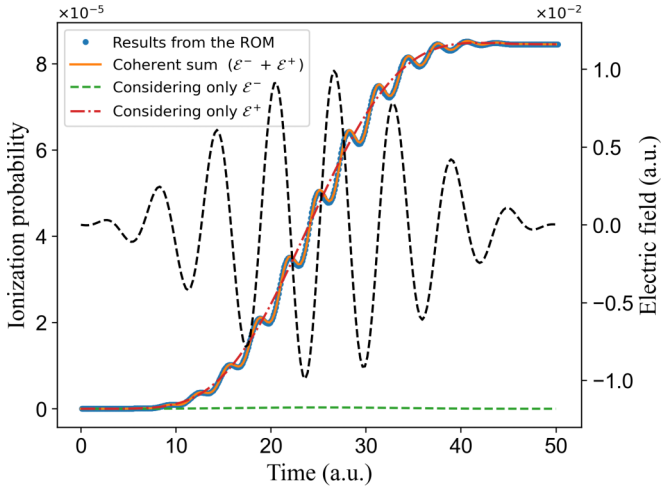

FIG. 3. Plot of the ionization probability as a function of time obtained by the first-order time-dependent theory defined by Eq. (20). The results are presented in full orange line. The dashed green distribution is obtained only considering the rotating wave approximation ($\mathcal{E}^-$) while the dot-dashed red curve corresponds to the case of the antirotation wave approximation ($\mathcal{E}^+$) which is expected to have a small contribution. For comparison, we have added the result obtained from the TDSE and the ROM (as in Fig. 2) in dotted blue curve. It shows a good agreement.

the end of the interaction. It is also interesting to notice that the distribution is composed of stripes as the time evolves. These stripes appear at the time values in the vicinity of the zero of the electric field. In order to better visualize the time evolution, the results obtained in Fig. 1 have been integrated over energy from 0 to 1.0 a.u. The result is then the ionization probability [see Eq. (14)] as a function of time and is plotted in Fig. 2 in blue.

From this figure, we observe a regular increase of the ionization probability as well as oscillations at twice the frequency of the driving field. The result obtained by the ROM is confirmed by using the definition based on the BSP applied on the wave function expressed in the length gauge as explained in the previous section. The BSP result is presented by the orange curve and almost perfectly fits the one obtained by the ROM technique. The slight difference observed (less than 0.1%) is due to the well-known Lorentzian tail contribution inherent to the use of the ROM (see [22] and Appendix A for more details). The oscillations are due to the well-known phenomenon of a sharp increase of the ionization probability when the amplitude of the field is maximal. There is still a puzzling feature which appears in the temporal evolution of the ionization probability, namely, the small decrease after each maximum. If one describes the ionization probability as the solution of a rate equation, having a rate that is always positive, such a decrease should not be obtained and "ladderlike" steps would have been the obtained result. From the physical point of view the fact that the rate is always positive implies that the ionization process is described by an irreversible process. In particular, the coherent aspect of the photoionization process is not included in rate equations. In order to further study these issues, we have performed the computation of the ionization probability in the frame of the first-order time-dependent theory in the length gauge for the reason already mentioned in the first section. The expression of the energy resolved ionization probability is

$$\mathcal{P}(E,t) = \left| \int_0^t e^{iE\tau} \langle E|\mathcal{E}(\tau)\cdot \boldsymbol{r}|\varphi_0\rangle e^{-iE_0\tau} d\tau \right|^2, \tag{20}$$

with $|\varphi_0\rangle$ and $|E\rangle$ being the ket of the initial state and in the continuum, respectively.

The state $|E\rangle$ has been obtained by diagonalization of the field-free Hamiltonian and normalized to energy so that $\langle E|E'\rangle = \delta(E-E')$. The resulting dipole $\langle E|\mathcal{E}(\tau)\cdot \boldsymbol{r}|\varphi_0\rangle$ has then been fitted to the sum of two exponential decay functions. The results obtained after integration over energy are presented in Fig. 3. First, one can notice the very good agreement with the results obtained by the TDSE presented in Fig. 2. In particular, we reproduce the oscillations observed in the results obtained by the TDSE, showing that even this simple model is far from the results that would have been obtained with solving a rate equation. In order to understand the physical origin of these oscillations, we have computed the first-order perturbation theory in the rotating wave approximation. The field is decomposed into $\mathcal{E}(t) = \mathcal{E}^+(t) + \mathcal{E}^-(t)$ where $\mathcal{E}^+(t)$ is composed of the envelope times $e^{i\omega_0 t}$ and $\mathcal{E}^-(t)$ is the complex conjugate. We then define two amplitudes of transitions, associated with either the $\mathcal{E}^+(t)$ or $\mathcal{E}^-(t)$ operator that sum up coherently. The results, when only $\mathcal{E}^+$ or $\mathcal{E}^-$ is considered, are presented in green and orange lines in Fig. 3, respectively. The oscillations completely vanish and the distribution exhibits a monotonic evolution. The distribution related to the field $\mathcal{E}^-$ is the closest one as expected since this corresponds to the absorption process. The oscillation observed in the time-dependent ionization signal is then due to the interference between the amplitudes associated with the fields $\mathcal{E}^+$ and $\mathcal{E}^-$. This shows that removing the coherent

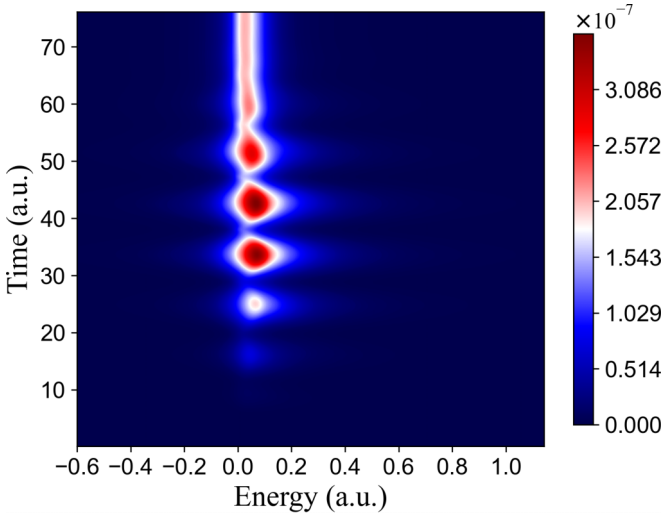

FIG. 4. Same as Fig. 1 but for the field defined by an amplitude of $\mathcal{E}_0 = 3.3 \times 10^{-3}$ a.u., a central frequency of $\omega_0 = 0.33$ a.u., and a pulse duration of four cycles.

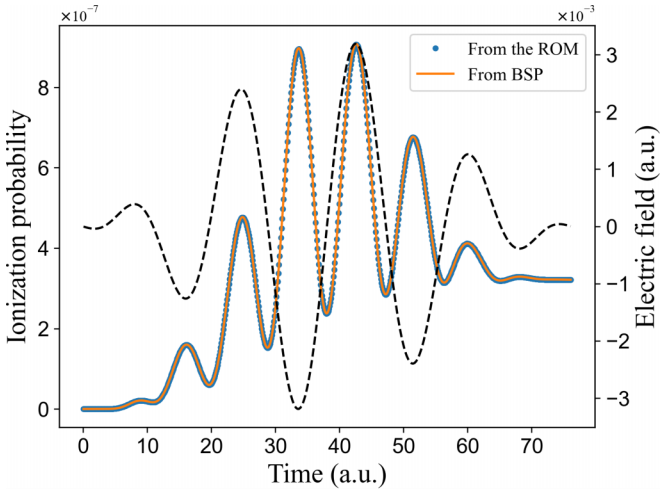

FIG. 5. Same as Fig. 2 but for the field defined by an amplitude of $\mathcal{E}_0 = 3.3 \times 10^{-3}$ a.u., a central frequency of $\omega_0 = 0.33$ a.u., and a pulse duration of four cycles.

properties of the ionization process leads to inaccurate description of the dynamics.

As an illustration we also provide in the Supplemental Material [29] the plot showing the gauge dependence of the ionization probability as provided by $\int_{E>0} dE \langle \Psi_{\mathfrak{g}}(t)|R_{H_0}(E)|\Psi_{\mathfrak{g}}(t)\rangle$. According to Sec. II the results are expected to be different except for the time for which the vector potential is zero (see also for instance [30,31]). This is in particular true at the beginning and at the end of the interaction in accordance with the fact that there is gauge invariance of the photoionization probability. According to our analysis, only the distribution related to the projection on the wave function expressed in the length gauge [see Eq. (17)] is meaningful and corresponds to the actual time-dependent ionization probability that can be used for further analysis as explained in the introduction. We show also in the Supplemental Material [29] the results obtained for the multiphoton and tunneling cases as detailed below. The results lead to the same conclusion as for the linear case but show a more drastic difference between the two gauges.

B. Multiphoton regime

In this section, we study the nonlinear regime and set the central frequency of the laser to $\omega_0 = 0.33$ a.u. ($\lambda = 138$ nm) and an amplitude of the vector potential to 0.01 a.u. as in the linear case (the corresponding electric field is $\mathcal{E}_0 = 3.3 \times 10^{-3}$ a.u. and laser intensity is $I_0 = 3.8 \times 10^{11}$ W/cm^2). The total number of cycles describing the field is set to 4. The ionization probability resolved in energy and time is provided in Fig. 4.

The obtained distribution is very different than the one presented in the linear regime. It exhibits stripes almost independent of energy. These stripes oscillate at twice the frequency of the laser with a very strong contrast (almost 80%). By integrating over energy the distribution obtained by the ROM, one gets the ionization probability as a function of time that is plotted in Fig. 5.

Comparing the time evolution of the ionization probability with the evolution of the electric field (dashed black curve of Fig. 5) we remark that the maximum of the ionization probability is reached at each extremum of the electric field. This evolution is in contrast to the linear case, and also differs drastically to what is expected from the solution that would have been obtained by solving a rate equation.

C. Tunneling regime

The last configuration corresponds to the tunneling regime. In that case, the field has a central frequency $\omega_0 = 0.07$ a.u. ($\lambda = 655$ nm), a field amplitude of $\mathcal{E}_0 = 0.14$ a.u. ($I_0 = 6.9 \times 10^{14}$ W/cm^2), and a pulse duration of four cycles. The box size is set to $x_{\max} = 500$ a.u., $dx = 0.5$ a.u., and $\epsilon = 5 \times 10^{-3}$ a.u. The ponderomotive energy is then $U_p = 1$ a.u. and the Keldysh parameter is $\gamma = 0.57 < 1$ defining conditions corresponding to the tunneling regime. The plot of the time and energy-dependent ionization spectra is provided in Fig. 6. The integration over energy is compared to the ionization probability resulting from the bound-state subtraction in Fig. 7. An excellent agreement is obtained showing the confidence in the ROM analysis. In particular, it does not show the expected ladderlike distribution that would have been obtained from solving a rate equation. The rate equation was expected to be in a better agreement as compared to linear and multiphoton cases since we are in the tunneling regime where the photon frequency should play a less important role.

The results differential in energy depicted in Fig. 6 show a rich and complex structure. The interference pattern is due to the above threshold ionization peaks that build up as the number of cycles increases [32]. The first release of the wave packet corresponds to an evolution in the range of time from 120 to 150 a.u. This wave packet is born at 120 a.u. of time, so at the maximum of the electric field with an energy spread localized near 0 eV. This is the usual image evoked in the tunneling regime. Then the wave packet evolves and comes back in the vicinity of the ion. Unfortunately, this space-dependent aspect of the dynamics is out of reach. This first feature,

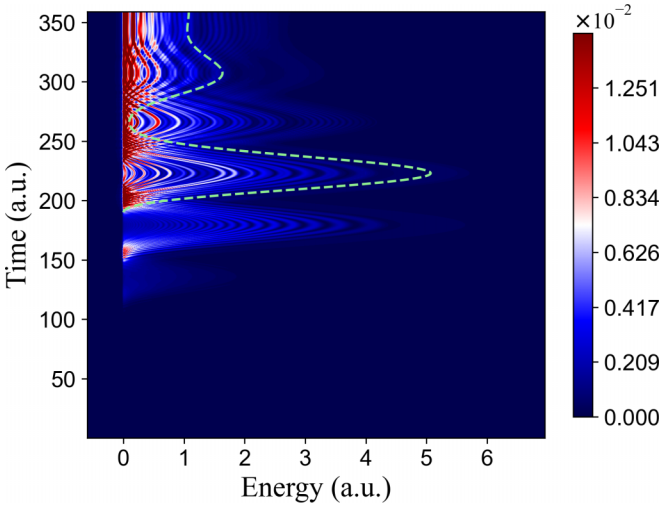

FIG. 6. Same as Fig. 1 but for the field defined by an amplitude of $\mathcal{E}_0 = 0.14$ a.u., a central frequency of $\omega_0 = 0.07$ a.u., and a pulse duration of four cycles. The green dashed curve corresponds to the time evolution of the energy of the classical trajectory associated with a birth time of 190 a.u. and zero momentum as discussed in the text.

representing the dynamics of the first released wave packet, does not contain any stripes and shows an energy cutoff of about 0.5 to 1 a.u. Then the field releases a second wave packet at time 150 a.u. which interferes with the first wave packet leading to the complex interference pattern observed at the second oscillation. The wave packet then continues to evolve and shows a more and more complex structure as the number of released wave packet increases. The dynamics of the wave packet reaching the maximum energy at time 223 a.u. exhibits an extent of the wave packet with an energy cutoff at 2 a.u. and a slow amplitude decrease up to an energy of 5 a.u. At this value of the field, the instantaneous U_p is 1 a.u. While the extension of the PES of the direct electron goes up to $2U_p$ [33] at the end of the pulse, we clearly observe an extent of the PES up to $5U_p$ during the interaction. This can be

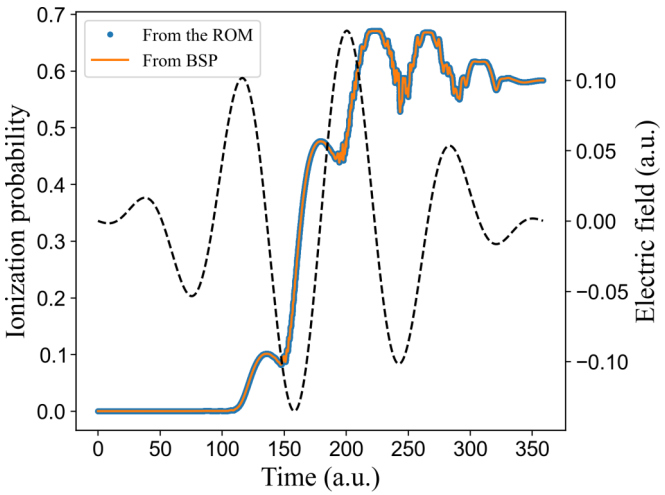

FIG. 7. Same as Fig. 2 but for the field defined by an amplitude of $\mathcal{E}_0 = 0.14$ a.u., a central frequency of $\omega_0 = 0.07$ a.u., and a pulse duration of four cycles.

understood classically from momentum conservation giving rise to $p(t) = A(t) - A(t_0)$ [assuming $p(t_0) = 0$] with $p(t)$ the classical momentum and t_0 the time at which the wave packet is released. The highest probability to release the wave packet corresponds to times t_0 close to maxima of the electric field for which $A(t_0)$ is zero leading to a maximum energy of $2U_p$ as observed in our results at time 220 a.u.

We now focus on the part of the wave packet having an energy extent up to $5U_p$. From the classical picture we are then interested in the value of $p(t)$ so that $p(t) = \sqrt{2E} = \sqrt{2 \times 5U_p} = \sqrt{5/2}A_0$. Since this energy is obtained at the time t so that $A(t) = A_0$ then we seek for the time t_0 for which $|A_0 - A(t_0)| = \sqrt{5/2}A_0$. From this relation, we deduce a contribution of the initial wave packet having a birth time satisfying $A(t_0) \approx -0.6A_0$ giving a time t_0 of about 190 a.u. This corresponds to an electric-field amplitude which is half its maximal amplitude. Having defined this initial conditions, from Newton's laws of motion only including the interaction with the laser field, we can retrace the classical trajectory and plot the associated energy as a function of time. The result is presented by the dashed green curve in Fig. 6 and shows good agreement with the TDSE simulations. This wave-packet contribution ends up at an energy of U_p at the end of the pulse as shown in our simulations. This plot does not present the contribution of the recollision [33] leading to a high-energy plateau since it is a linear scale and the plateau due to recollision located in the energy range from $2U_p$ up to $10U_p$ shows up at a much lower probability. It can be studied also in detail with our theory but it is going beyond the scope of this paper and would require the use of the resolvent method of fourth order as detailed in Appendix A.

IV. NONDIPOLE CASE

Up to now, we have considered the interaction of the laser pulse with the system in the frame of the dipole approximation. Can the formalism presented in the first section be extended to the case of nondipole description of the field? In order to answer this question, we need a description of the laser-matter interaction that is defined by a unitary transformation so that $H(t) = TH_0T^\dagger$ with $T = e^{-i\chi(\boldsymbol{r},t)}$. This general formulation of the Hamiltonian describing the interaction with the field, as demonstrated in Sec. II, has a spectrum which is the same as the one defined for the field-free case. The Hamiltonian is then the one provided by setting $\phi = 0$ [see Eqs. (1) and (2)] and in its minimal coupling so only including the transverse component of the vector potential so that $\boldsymbol{A}(\boldsymbol{r}, t) = \boldsymbol{A}_\perp(\boldsymbol{r}, t)$. As a reminder, this choice of the potentials also belongs to the Lorentz gauge. The corresponding relation between the vector potential and χ is then $\boldsymbol{\nabla}\chi = \boldsymbol{A}_\perp(\boldsymbol{r}, t)$. If there is such a solution, the magnetic component is provided by $\mathcal{B}(\boldsymbol{r}, t) = \boldsymbol{\nabla} \times \boldsymbol{A}_\perp(\boldsymbol{r}, t) = \boldsymbol{\nabla} \times \boldsymbol{\nabla}\chi = \boldsymbol{0}$. In conclusion, by virtue of *reductio ad absurdum* there is no solution for $\boldsymbol{\nabla}\chi = \boldsymbol{A}_\perp(\boldsymbol{r}, t)$ except in the dipole approximation in which case the vector potential is irrotational. This is coming from the fact that the transverse component of the vector potential remains unchanged by gauge transformation since it is the one leading to the magnetic component which is a gauge invariant quantity. Consequently, there is no possibility to extract a meaningful time-dependent ionization probability in

the nondipole description of the field, despite the fact that the PES are gauge invariant at the end of the interaction.

V. GAUGE TRANSFORMATION WHEN SOLVING THE TDSE IN A SUBSPACE

So far, calculations are performed using the full eigenbasis defined by the Hamiltonian. This leads to the property of closure relation for instance. In some situations, the use of a restricted subspace of the Hamiltonian appears necessary. This is the case when using the SAEA where the lowest energetic states correspond to orbitals that are filled up and should not be populated during the propagation. While removing these states using the spectral method does not present any difficulty, when using a propagation method in real space, the so-called grid method, it requires special care. To do so, we use the Feshbach [34,35] formalism so that the full space represented by the eigenstate of the Hamiltonian is split into two orthogonal subspaces denoted $\mathfrak{P}$ and $\mathfrak{Q}$. The subspace $\mathfrak{P}$ contains the states of interest and $\mathfrak{Q}$ contains the ones that are disregarded. Of course $\mathfrak{P}$ and $\mathfrak{Q}$ are complementary and satisfy $\mathbf{1} = \mathfrak{P} + \mathfrak{Q}$ and $\mathfrak{P}\mathfrak{Q} = \mathfrak{Q}\mathfrak{P} = 0$. The propagation using the grid method is then performed in the Hamiltonian $\mathfrak{P}H\mathfrak{P}$. This is what is also performed formally speaking when removing the states in the spectral method. The situation is now to find the consequences of the gauge transformation within this subspace. To that purpose, we define the new Hamiltonian as $\tilde{H}_{\mathfrak{g}} = \mathfrak{P}H_{\mathfrak{g}}\mathfrak{P}$ in the gauge $\mathfrak{g}$. We start from the general transformation applied on H

$$H_{\mathfrak{g}'} = UH_{\mathfrak{g}}U^{\dagger} + iU^{\dagger}\frac{\partial}{\partial t}U \tag{21}$$

and we then project on the subspace $\mathfrak{P}$:

$$\mathfrak{P}H_{\mathfrak{g}'}\mathfrak{P} = \mathfrak{P}UH_{\mathfrak{g}}U^{\dagger}\mathfrak{P} + i\mathfrak{P}U^{\dagger}\frac{\partial}{\partial t}U\mathfrak{P}. \tag{22}$$

We seek for a gauge transform which keeps the Hamiltonian in the subspace defined by $\mathfrak{P}$, which means that U commutes with $\mathfrak{P}$. It then leads to

$$\mathfrak{P}H_{\mathfrak{g}'}\mathcal{P} = U\mathfrak{P}H_{\mathfrak{g}}\mathfrak{P}U^{\dagger} + i\mathfrak{P}U^{\dagger}\frac{\partial}{\partial t}U\mathfrak{P}. \tag{23}$$

If we now write $U = \exp(-i\chi)$, then

$$\mathfrak{P}H_{\mathfrak{g}'}\mathfrak{P} = U\mathfrak{P}H_{\mathfrak{g}}\mathfrak{P}U^{\dagger} + \mathfrak{P}\frac{\partial\chi}{\partial t}\mathfrak{P}. \tag{24}$$

From this expression we clearly see that by replacing χ by $\tilde{\chi} = \mathfrak{P}\chi\mathfrak{P}$, we retrieve a solution that satisfies all the necessary conditions. In conclusion the gauge transformation is acting through the operator $U = \exp(-i\mathfrak{P}\chi\mathfrak{P})$. In particular, the transformation going from velocity to length form is written $\exp(i\boldsymbol{A}(t)\cdot\mathfrak{P}\mathrm{R}\mathfrak{P})$ in the dipole description of the field. What is the consequence for the determination of time-dependent ionization probability? As detailed in the previous sections, we seek for a transformation of the form $\mathfrak{P}H_{\mathfrak{g}}\mathfrak{P} = T\mathfrak{P}H_0\mathfrak{P}T^{\dagger}$ in order to conserve an identical spectrum of $\mathfrak{P}H\mathfrak{P}$ and $\mathfrak{P}H_0\mathfrak{P}$ at all times. We start from the known transformation in velocity gauge $\mathfrak{P}H_V\mathfrak{P} = \mathfrak{P}T_0H_0T_0^{\dagger}\mathfrak{P}$ with $T_0 = e^{-i\boldsymbol{A}(t)\cdot\boldsymbol{r}}$. Since $\mathfrak{P}$ and T_0 do not commute in general, we cannot obtain the transformation we seek for and all the conclusions we have drawn so far fall down in the restricted subspace. This conclusion is more general than the one affecting the PES since there is not, in general, gauge invariance even for the computation of the current—or dipole—in the subspace defined in this section. This is due do the noncommutativity of $\mathbf{R}$ and $\mathfrak{P}\chi\mathfrak{P}$.

There are three forms of the dipole response of the system: (i) the length form provided by $\langle\Psi|\mathbf{R}|\Psi\rangle$, (ii) the velocity form written $\langle\Psi|\boldsymbol{\Pi}(t)|\Psi\rangle$ with $\boldsymbol{\Pi}(t)$ the generalized momentum (see Sec. II), and (iii) the acceleration form $\langle\Psi|\nabla V(\mathbf{r})|\Psi\rangle$. In standard quantum mechanics they are all related by time derivative in relation with the Ehrenfest theorem. This is due to the properties $[\mathbf{R}, H] = -i\boldsymbol{\Pi}$ and $[\boldsymbol{\Pi}, H] = i\nabla V(\mathbf{r})$. From these formulas one can show the gauge invariance of the latter quantities. Since we have to deal with the Hamiltonian in a subspace, we have to replace H by $\mathfrak{P}H\mathfrak{P}$ and the corresponding gauge transformation. There is not a general commutative property of the operator by the gauge transform and in particular only the configuration involving the linearly polarized field and computing the dipole in the length form provides gauge invariance of the results.

VI. CONCLUSION

In this paper we have described the issue of gauge variance of the time-dependent ionization probability. We have made use of the resolvent methodology to show (1) that the spectrum defined by the field-free Hamiltonian is the same as the one defined in the velocity form and (2) that from this definition we can establish a procedure to obtain the energy distribution as a function of time. From conclusion 1 we can define unambiguously the region of energy for which ionization is meaningful. This energy definition can be transformed into a projection on bound states when the length form is used. This definition is particularly convenient and can be used to compare with other methodologies in order to discriminate the best ones. Clearly, from the three configurations investigated in this paper, a usual rate equation, despite a good formulation of the ionization probability at the end of the pulse, is incapable of reproducing the proper dynamics even in the simple cases. We have also determined a formulation of the gauge transformation in case of the TDSE resolved in a subspace. This formulation is quite different from what one would infer using the simple Goepper-Mayer transformation. Finally we concluded that an extension of this study cannot be performed in the nondipole case. Most of the study has been performed in one dimension, but its extension to full dimension does not present any conceptual difficulties. Special care has been made for multielectron extension. While full ionization probability can be performed by means of the resolvent as performed in this paper, the multichannel aspect of the physical insight might bring some difficulties.

ACKNOWLEDGMENTS

Computations were performed using high-performance computing resources from the Mésocentre de Calcul Intensif Aquitain of the Université de Bordeaux and of the Université de Pau et des Pays de l'Adour. Financial support was obtained from the Ministry of Education, Youth and Sports within the targeted support of "Large

infrastructures" (Project No. LM2018141). This work was also supported by the project "Advanced research using high intensity laser produced photons and particles" (Grant No. CZ.02.1.01/0.0/0.0/16_019/0000789) and by the European Regional Development Fund (ADONIS) and Grantová agentura České republiky (GACR Grant No. 20-24805J).

APPENDIX A: PROPERTIES OF THE RESOLVENT OPERATOR

In this Appendix we recall a few properties of the resolvent operator that has been extensively described in [21,22].

The resolvent operator originally stems from the formal definition of the scattering amplitude related to ionization. Let us denote $|\Psi(T_f)\rangle$ the wave function obtained at the end of the pulse $\tau = T_f$. In order to obtain the amplitude of transition corresponding to ionization, one has to let the wave function propagate in time up to infinity and project onto plane waves leading to the amplitude of transition: $t(\mathbf{k}) = \lim_{\tau\to\infty}\langle\mathbf{k}|\Psi(T_f+\tau)\rangle$ where $|\mathbf{k}\rangle$ is a plane wave and $|\Psi(T_f+\tau)\rangle = U(\tau)\Psi(T_f)$ with $U(\tau)$ being the evolution operator associated with the field-free Hamiltonian H_0. Using the Møller operator [36], one can show that this amplitude of transition is formally provided by $t(\mathbf{k}) = \langle\Phi^-(\mathbf{k})|\Psi(T_f)\rangle$ where $|\Phi^-(\mathbf{k})\rangle$ is the eigenstate of H_0 having the proper incoming properties and normalized in energy. One can also use the Gell-Mann and Goldberger definition of $\lim_{\tau\to\infty}$ used in the amplitude of transition so that $t(\mathbf{k}) = \lim_{\epsilon\to 0^+}\langle\mathbf{k}|\frac{i\epsilon}{H_0-E-i\epsilon}|\Psi(T_f)\rangle$ with $E = k^2/2$ [37]. The probability of ionization is then $P_{\text{ion}} = \int d\mathbf{k} t^*(\mathbf{k})t(\mathbf{k}) = \lim_{\epsilon\to 0^+}\langle\Psi(T_f)|R(E,H_0)|\Psi(T_f)\rangle$ where $R(E,H_0) = \frac{\epsilon^2}{(H_0-E)^2+\epsilon^2}$ is the resolvent operator. While this expression is formally correct, its use requires some care since a finite box is employed to solve the TDSE as well as a finite value of ϵ. In these conditions, the resolvent operator is written $R(E,H_0) = N_{\epsilon,n}\frac{\epsilon^2}{(H_0-E)^2+\epsilon^2}$.

One can note that the use of the resolvent allows for the computation of the ionization probability without having to compute explicitly the eigenstates. A generalization of the resolvent operator is written

$$R_H(E) = N_{\epsilon,n}\frac{\epsilon^{2n}}{(E-H)^{2n}+\epsilon^{2n}}, \tag{A1}$$

where E is an energy (here a parameter of the resolvent), H a time-independent Hamiltonian, ϵ is a parameter related to the energy resolution of the resolvent, and $N_{\epsilon,n}$ is a constant coefficient allowing for converting probability into density probability (see [22] for more details and the explicit expression of $N_{\epsilon,n}$). The last coefficient n is related to the order as it will be detailed below. There is a range of ϵ for which the latter quantity becomes independent of it; this is the range of ϵ that should be employed and it is related to the density of states defined in the numerical box [21,22].

If we assume that the Hamiltonian is described by the set of eigenstates $|E_n\rangle$ associated with the energies E_n the resolvent is written

$$R_H(E) = \sum_k N_{\epsilon,n,k}\frac{\epsilon^{2n}|E_k\rangle\langle E_k|}{(E-E_k)^{2n}+\epsilon^{2n}} \tag{A2}$$

in this basis. $N_{\epsilon,n,k} = 1$ if k refers to a bound state and it is the k independent coefficient provided in [22] if k refers to a continuum state. We observe that the resolvent acts as a window function having an energy width depending on ϵ and n. In particular since only a range of ϵ defines the density of probability if one wants to increase the energy resolution then n becomes the only parameter and has to be increased.

The probability of populating a state of energy E then results from the contributions of states in its vicinity and the one more distant. The contribution of a specific state i is then

$$P = |c_i|^2\frac{\epsilon^{2n}}{(E-E_i)^{2n}+\epsilon^{2n}}, \tag{A3}$$

for which we have omitted the normalization coefficient $(N_{\epsilon,n,k})$ since we consider states in the continuum for which this coefficient is the same. This probability presents a long tail distribution provided by $\frac{\epsilon^{2n}}{(E-E_i)^{2n}}$ since $|E-E_i| > \epsilon$. This distribution can compete with the actual probability at the energy E. In order to avoid this situation we need to satisfy $|c_i|^2\frac{\epsilon^{2n}}{(E_j-E_i)^{2n}} < |c_j|^2$ so $\frac{|c_j|^2}{|c_i|} < (\frac{\epsilon}{E_j-E_i})^{2n}$ where $|c_j|$ is the probability at the energy $E = E_j$, the reference energy point for the demonstration. Since ϵ is set within an energy range to ensure the right properties of the resolvent, the remaining parameter that can be changed to increase the precision is n, and the larger n the better. In practice $n = 2$ is usually enough to describe most of the physics but increases the computational time [33].

APPENDIX B: ON THE DEFINITION OF THE ADIABATIC STATES FOR THE TIME-DEPENDENT HAMILTONIAN

In this Appendix we detail the concept of the adiabatic state for the time-dependent Hamiltonian as used in this paper. It is organized as follows: (i) we demonstrate how to define the adiabatic state, (ii) we give a physical interpretation of the latter state, and (iii) we illustrate the two previous points in the case of the Volkov state. We start by questioning if there exists a gauge leading to a time-dependent Hamiltonian having the same spectrum as the one of the field-free Hamiltonian.

We begin with the eigenproblem $H_0|\Psi_E\rangle = E|\Psi_E\rangle$ with $|\Psi_E\rangle$ being the eigenstate of H_0 associated with the eigenenergy E. We now write the operator of gauge transformation as $T(t)$ which is time dependent. We apply $T(t)$ on both sides of the eigenequation and get $T(t)H_0|\Psi_E\rangle = ET(t)|\Psi_E\rangle = T(t)H_0T^\dagger(t)T(t)|\Psi_E\rangle$. So the state $T(t)|\Psi_E\rangle$ is the eigenstate of $T(t)H_0T^\dagger(t)$ for the energy E, which is the eigenenergy of the stationary state $|\Psi_E\rangle$. This property is satisfied for the whole spectrum of eigenenergies, bound and continuum states, and is valid at all times. So the question is now to determine if whether a Hamiltonian representing the interaction with an electromagnetic field can be represented by a Hamiltonian of the form $H(t) = T(t)H_0T^\dagger(t)$. As described in the paper there is such a Hamiltonian in the dipole approximation which is the velocity gauge and $T(t)$ is provided by $e^{-i\mathbf{A}(t)\cdot\mathbf{r}}$. From the latter theorem, we can define a state $T(t)|\Psi_E\rangle$, that is the eigenstate associated with a constant eigenenergy E, for the time-dependent Hamiltonian $T(t)H_0T^\dagger(t)$. That is the reason why we call this state the adiabatic state. The

time-dependent property is then completely transferred into the wave function. To give an illustration of this property, we will start from the Volkov state written in the velocity gauge, corresponding to the solution of the time-dependent Schrödinger equation for which the potential $V(\boldsymbol{r})$ [see Eq. (1)] is set to zero. The Volkov state $\Psi_{VV}(t) = \frac{1}{(2\pi)^{3/2}} e^{i\int d\tau [\mathbf{k}+\mathbf{A}(\tau)]^2/2 + i\mathbf{k}\cdot\mathbf{r}}$ is the solution of the TDSE $H_V(t)|\Psi_{VV}(t)\rangle = i\frac{\partial}{\partial t}|\Psi_{VV}(t)\rangle$ in the velocity gauge. Starting from a plane-wave solution of the field-free Hamiltonian with the energy $E = \frac{k^2}{2}$ noted $|E\rangle$ and using the transformation defining the adiabatic state of the time-dependent Hamiltonian, we get $\frac{1}{(2\pi)^{3/2}} e^{i[\mathbf{k}-\mathbf{A}(t)]\cdot\mathbf{r}}$. It is easy to check that this state is the eigenstate of the operator $\frac{[\mathbf{p}+\mathbf{A}(t)]^2}{2}$, that is the Hamiltonian in the velocity gauge, for the constant energy $E = \frac{k^2}{2}$. Last, we emphasize that, in contrast to the Volkov state, the adiabatic state is not a solution of the TDSE.

[1] J. A. Sobota, Y. He, and Z.-X. Shen, Rev. Mod. Phys. **93**, 025006 (2021).

[2] M. Waitz, R. Y. Bello, D. Metz, J. Lower, F. Trinter, C. Schober, M. Keiling, U. Lenz, M. Pitzer, K. Mertens, M. Martins, J. Viefhaus, S. Klumpp, T. Weber, L. Ph. H. Schmidt, J. B. Williams, M. S. Schöffler, V. V. Serov, A. S. Kheifets, L. Argenti, A. Palacios, F. Martín, T. Jahnke, and R. Dörner, Nat. Commun. **8**, 2266 (2017).

[3] G. Mainfray and G. Magnus, Rep. Prog. Phys. **54**, 1333 (1991).

[4] X. F. Li, A. L'Huillier, M. Ferray, L. A. Lompré, and G. Mainfray, Phys. Rev. A **39**, 5751 (1989).

[5] P. Agostini and L. F. DiMauro, Rep. Prog. Phys. **67**, 813 (2004).

[6] M. Schultze, M. Fieß, N. Karpowicz, J. Gagnon, M. Korbman, M. Hofstetter, S. Neppl, A. L. Cavalieri, Y. Komninos, Th. Mercouris, C. A. Nicolaides, R. Pazourek, S. Nagele, J. Feist, J. Burgdörfer, A. M. Azzeer, R. Ernstorfer, R. Kienberger, U. Kleineberg, E. Goulielmakis, F. Krausz, and V. S. Yakovlev, Science **328**, 1658 (2010).

[7] K. Klünder, J. M. Dahlström, M. Gisselbrecht, T. Fordell, M. Swoboda, D. Guénot, P. Johnsson, J. Caillat, J. Mauritsson, A. Maquet, R. Taïeb, and A. L'Huillier, Phys. Rev. Lett. **106**, 143002 (2011).

[8] J. M. Dahlström, D. Guénot, K. Klünder, M. Gisselbrecht, J. Mauritsson, A. L'Huillier, A. Maquet, and R. Taïeb, Chem. Phys. **414**, 53 (2013).

[9] J. Vos, L. Cattaneo, S. Patchkovskii, T. Zimmermann, C. Cirelli, M. Lucchini, A. Kheifets, A. S. Landsman, and U. Keller, Science **360**, 1326 (2018).

[10] S. Grundmann, D. Trabert, K. Fehre, N. Strenger, A. Pier, L. Kaiser, M. Kircher, M. Weller, S. Eckart, L. Ph. H. Schmidt, F. Trinter, T. Jahnke, M. S. Schöffler, and R. Dörner, Science **370**, 339 (2020).

[11] A. Sopena, A. Palacios, F. Catoire, H. Bachau, and F. Martín, Commun. Phys. **4**, 253 (2021).

[12] H. Bachau, M. Dondera, and V. Florescu, Phys. Rev. Lett. **112**, 073001 (2014).

[13] A. Galstyan, O. Chuluunbaatar, A. Hamido, Yu. V. Popov, F. Mota-Furtado, P. F. O'Mahony, N. Janssens, F. Catoire, and B. Piraux, Phys. Rev. A **93**, 023422 (2016).

[14] D. Bauer, D. B. Milosevic, and W. Becker, Phys. Rev. A **72**, 023415 (2005).

[15] M. Uiberacker, Th. Uphues, M. Schultze, A. J. Verhoef, V. Yakovlev, M. F. Kling, J. Rauschenberger, N. M. Kabachnik, H. Schröder, M. Lezius, K. L. Kompa, H.-G. Muller, M. J. J. Vrakking, S. Hendel, U. Kleineberg, U. Heinzmann, M. Drescher, and F. Krausz, Nature (London) **446**, 627 (2007).

[16] J. Derouillat, A. Beck, F. Pérez, T. Vinci, M. Chiaramello, A. Grassi, M. Flé, G. Bouchard, I. Plotnikov, N. Aunai, J. Dargent, C. Riconda, and M. Grech, Comput. Phys. Commun. **222**, 351 (2018).

[17] H. Jouin, M. Raynaud, G. Duchateau, G. Geoffroy, A. Sadou, and P. Martin, Phys. Rev. B **89**, 195136 (2014).

[18] Y. H. Lai, J. Xu, U. B. Szafruga, B. K. Talbert, X. Gong, K. Zhang, H. Fuest, M. F. Kling, C. I. Blaga, P. Agostini, and L. F. DiMauro, Phys. Rev. A **96**, 063417 (2017).

[19] I. A. Ivanov, C. Hofmann, L. Ortmann, A. S. Landsman, C. H. Nam, and K. T. Kim, Commun. Phys. **1**, 81 (2018).

[20] X. M. Tong and C. D. Lin, J. Phys. B: At. Mol. Opt. Phys. **38**, 2593 (2005).

[21] K. J. Schafer and K. C. Kulander, Phys. Rev. A **42**, 5794 (1990).

[22] F. Catoire and H. Bachau, Phys. Rev. A **85**, 023422 (2012).

[23] F. Catoire, R. E. F. Silva, P. Rivière, H. Bachau, and F. Martín, Phys. Rev. A **89**, 023415 (2014).

[24] P. Wopperer, U. De Giovannini, and A. Rubio, Eur. Phys. J. B **90**, 51 (2017).

[25] D. Gaspard, J. Math. Phys. **59**, 112104 (2018).

[26] R. G. Newton, J. Math. Phys. **1**, 319 (1960).

[27] I. Gohberg, S. Goldberg, and M. A. Kaashoek, *Classes of Linear Operators* (Springer, New York, 1990), Vol. 1, Chap. I.2.

[28] G. Göppert-Mayer, Ann. Phys. (NY) **401**, 273 (1931).

[29] See Supplemental Material at http://link.aps.org/supplemental/10.1103/PhysRevA.106.053115 for additional plots.

[30] E. Cormier and P. Lambropoulos, J. Phys. B: At. Mol. Opt. Phys. **29**, 1667 (1996).

[31] S. Hutchinson, M. A. Lysaght, and H. W. van Der Hart, J. Phys. B: At. Mol. Opt. Phys. **43**, 095603 (2010).

[32] P. Agostini, F. Fabre, G. Mainfray, G. Petite, and N. K. Rahman, Phys. Rev. Lett. **42**, 1127 (1979).

[33] P. Colosimo, G. Doumy, C. I. Blaga, J. Wheeler, C. Hauri, F. Catoire, J. Tate, R. Chirla, A. M. March, G. G. Paulus, H. G. Muller, P. Agostini, and L. F. DiMauro, Nat. Phys. **4**, 386 (2008).

[34] H. Feshbach, Ann. Phys. (NY) **5**, 357 (1958).

[35] H. Feshbach, Ann. Phys. (NY) **19**, 287 (1962).

[36] C. Møller, Mat. Fys. Medd. **23**, 1 (1945).

[37] M. Gell-Mann and M. L. Goldberger, Phys. Rev. **91**, 398 (1953).